

# ULTRASONIC AIR-BORNE PROPULSION THROUGH SYNTHETIC JETS

Hai Liu\*, Akash Roy, Yongkui Tang, Matin Barekatain and Eun Sok Kim

Department of Electrical and Computer Engineering  
University of Southern California, Los Angeles, California, USA

## ABSTRACT

This paper presents acoustic propulsion in air by synthesis jets produced by ultrasounds. Various ultrasonic air-borne propellers have been fabricated on 0.37-mm-thick commercial card piezoelectric speakers (APS2513S-T-R,  $25.2 \times 16.6 \times 0.37$  mm $^3$  in size), and studied, with the propulsion force measured through a precision weight scale, as the orifice size, thickness, spacing between orifices, and number (in the orifice array) are varied. Also varied is the orifice depth profile, as the fabrication processes for the orifices produce varying profiles. Strongest acoustic propulsion of 5.4 mg is obtained at 66 kHz (far beyond audible range) with 14  $\times$  14 orifice array made on a 0.1-mm-thick polyester plate (resulting in a propeller of  $25.2 \times 16.6 \times 1.37$  mm $^3$  in volume and 500 mg in weight). The acoustic propulsion force, though 93 times less than the propeller weight, is capable of making the propeller jump and move laterally.

## INTRODUCTION

Synthetic air jet, a zero net mass flux with non-zero momentum, can be generated through a vibrating diaphragm in a cavity with orifice (Fig. 1a), and can be used for propulsion, thermal management, flow control, etc. [1-3]. Synthetic air jet produces more propulsion force at a lower frequency (with a higher wavelength) and has mostly been obtained with audible sounds (i.e.,  $<10$  kHz) [1-6], though a micro-machined synthetic jet actuator designed to work at ultrasonic frequencies has been reported without any measured propulsion force [7]. We earlier demonstrated air-borne acoustic propeller at audio frequency [8]. As the audible sound impacts nearby humans, we have explored synthetic jets in ultrasonic frequencies, and report our recent results on acoustic propulsion with ultrasounds, as we vary the orifice design and fabrication process. Also, reported is our experimental observation on the effects of temperature on propulsion force.

## EXPERIMENT

### Device

The propeller is built on a 0.37 mm thick commercial card piezoelectric speaker (APS2513S-T-R,  $25.2 \times 16.6 \times 0.37$  mm $^3$  in size) with an attached polyester sheet with orifices (Fig. 1b and Fig. 1c). The polyester cover sheet is attached to the speaker with a 0.9 mm thick tape, so that there is 0.9 mm air gap between the speaker and the cover sheet. Throughout the experiments, we have used sinusoidal signal of 20 V<sub>peak-to-peak</sub> to drive the speaker.

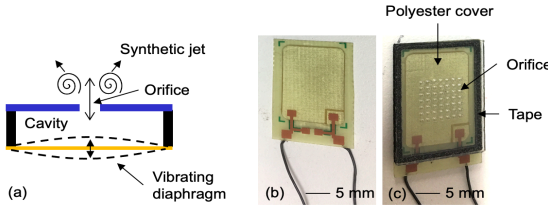


Figure 1: (a) Cross-sectional schematic of the synthetic jet generation, (b) photo of a piezoelectric card speaker, (c) photo of the acoustic propeller with the speaker and a laser-machined polyester cover with 7x7 orifices.

### Propulsion force measurement

To quantify the propulsion force precisely, the propeller is placed over a precision scale (METTLER TOLEDO MS104S/03 with 0.1 mg resolution) through a hollow adaptor with the propeller's orifices facing up for downward propulsion force (Fig. 2).

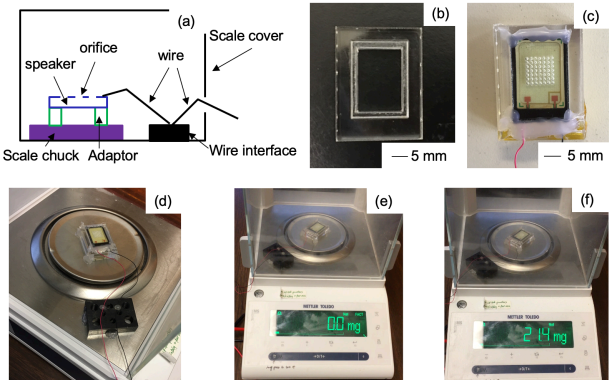


Figure 2: Propulsion force measurement through a precision weight scale: (a) schematic of the test set-up, (b) photo of the hollow adaptor, (c) photo of the acoustic propeller attached to the adaptor, (d) photo of the propeller (with the adaptor) on the scale along with the wire interface, (e) photo of the scale reading (0.0 mg) without power applied to the propeller, (f) scale reading (21.4 mg) with power applied to the propeller.

### Orifice design and fabrication process

Four orifice design parameters (orifice thickness, orifice diameter, orifice array size, and spacing between the orifices) at three levels are evaluated for the propulsion force (Table 1).

Table 1: Parameters and levels of the orifice design

Parameters	Levels		
	1	2	3
Orifice thickness ( $\mu\text{m}$ )	500	100	50
Orifice size ( $\mu\text{m}$ )	420	100	50
Array size	3x3	7x7	14x14
Spacing (mm)	0.6	1.2	1.8

Two processes are studied for orifice fabrication on polyester sheet: laser drilling without photolithography and O<sub>2</sub> reactive ion etching (RIE) with photolithography. Laser drilling can produce each orifice fast (though one at a time) but produces slanted sidewall, while RIE takes hours to make the orifices on a relatively thick substrate, though it produces vertical sidewall.

### Temperature measurement

The piezoelectric card speaker generates substantial amount of heat, at ultrasonic frequencies (though negligibly at audio frequencies for the same drive peak-to-peak voltage), and we have measured the temperature at the speaker with a point thermocouple (Fig. 3). The effect of the temperature rise on the propulsion force is

studied by operating the speaker with  $20V_{pp}$  continuously at 66 kHz for 10 seconds to raise the temperature to  $70^{\circ}\text{C}$  and then driving the speaker with various frequencies while the temperature at the speaker remains about  $70^{\circ}\text{C}$ .

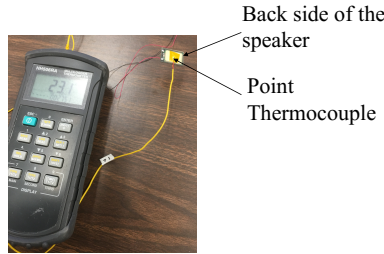


Figure 3: Temperature measurement at the card speaker, as the speaker is driven with various operating parameters.

## RESULTS AND DISCUSSION

### Impact of orifice design

Twenty-six legs of orifice design parameters have been studied for propulsion force with laser drilling process (Table 2). We list the highest propulsion force between 17 – 50 kHz as the most desirable output, because humans cannot hear sound beyond 17 kHz and since the temperature at the speaker increases fast beyond 50 kHz (though we have obtained propulsion force around 66 kHz).

Table 2: Matrix of orifice design

Leg#	Levels				Highest propulsion force (17 – 50 kHz) (mg)
	Thickness	Diameter	Array	Spacing	
1	1	2	3	2	2.4
2*	2	3	3	3	1.4
3	3	3	1	2	0
4	1	1	2	1	1.4
5	2	1	2	2	2.7
6	3	3	3	1	0
7	1	1	1	3	2.1
8	2	2	1	1	0
9	3	2	2	3	0
10	1	3	2	1	1.4
11	2	2	1	2	3.1
12*	3	1	3	3	0
13	3	3	2	2	0
14	3	3	2	1	0.7
15	3	2	2	2	2.9
16	3	1	2	2	0
17	2	1	2	2	2.6
18	2	2	2	2	2.7
19	2	3	2	2	0
20	2	2	1	3	1.3
21	1	1	2	2	0.8
22	2	2	2	2	2.6
23	2	2	1	2	2
24	2	2	3	2	1.1
25	2	2	1	3	0.7
26	2	2	2	3	3.7

\* The array size is  $10 \times 10$  with 1.5mm spacing between orifices in both orthogonal directions for Leg 2 and Leg 12 as there is not enough space on the polyester cover for Level 3 for both Array and Spacing.

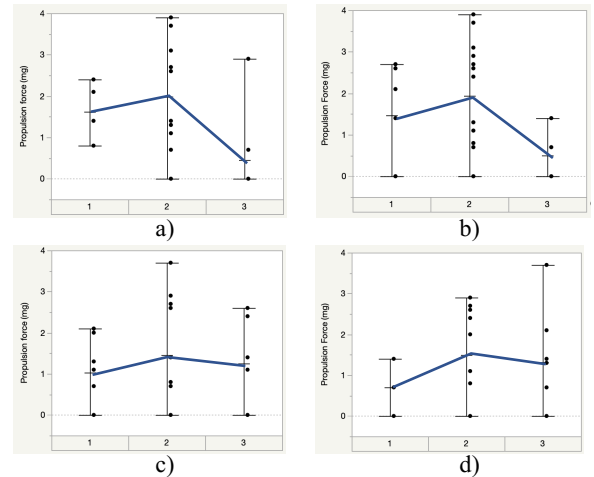


Figure 4: Measured propulsion forces vs orifice (a) thickness, (b) diameter, (c) array size, and (d) spacing.

According to the measured data shown in Fig. 4, the level 2 values for the orifice thickness, diameter, array size and space lead to higher propulsion force on the average. In general, a thicker orifice has higher acoustic resistance [4] and leads to a smaller propulsion force. However, when the orifice is too thin (e.g., 50  $\mu\text{m}$  in this study), the polyester sheet is so flexible that the sheet itself vibrates in response to applied sound pressure, resulting in a decrease in propulsion force. A smaller orifice can lead to a stronger propulsion force due to higher acoustic streaming effect near a smaller orifice. However, acoustic resistance increases as the diameter is reduced. Also, note that Fig. 4 is based on the experiments listed Table 2, and does not mean that the orifice with the mid-level of each factor necessarily has the highest propulsion force. Leg 26 (Fig. 5) has the highest propulsion force (3.7 mg) with frequency higher than 17 kHz and widest frequency range with propulsion force in all these 26 legs.

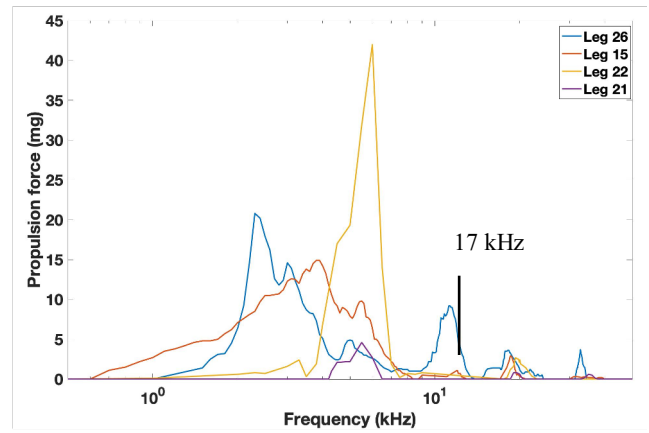


Figure 5: Measured propulsion force vs frequency for different orifice designs. Leg 26 (Table 2) produces acoustic propulsion around 20 kHz and 32 kHz with highest propulsion force 3.7 mg at 32.8 kHz.

Measured sound pressure levels of the speaker driven with  $20V_{pp}$  for different legs in Table 2 are shown in Fig. 6, and we find that the frequencies where the propulsion force is strong (whether in audio or ultrasound range) (Fig. 5) are not necessarily the frequencies where the sound pressure levels (measured with and without the orifice-containing cover) are high (Fig. 6), due to the orifice size and thickness affecting the synthetic jet generation.

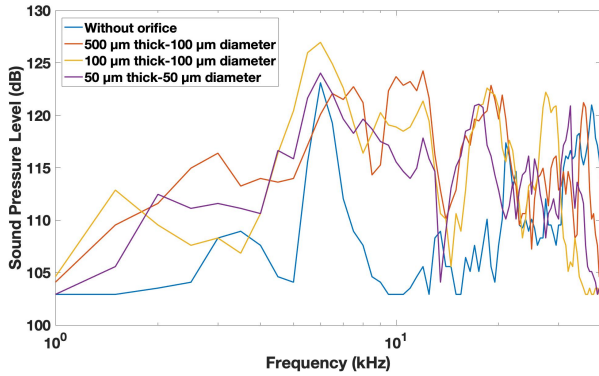


Figure 6: Open-field sound pressure level (in anechoic chamber) vs frequency without and with orifices.

### Effect of orifice fabrication process

We have fabricated  $100\text{ }\mu\text{m}$  thick orifices with  $50\text{ }\mu\text{m}$  and  $100\text{ }\mu\text{m}$  diameter on polyester sheet through oxygen RIE, following the steps illustrated in Fig. 7a. A  $0.2\text{ }\mu\text{m}$  thick sputter-deposited aluminum is used as an etch mask during RIE (Fig. 7a(i)). It takes about 9 hours to etch through the  $100\text{ }\mu\text{m}$  thick polyester with the  $\text{O}_2$  RIE at 250 Watt.

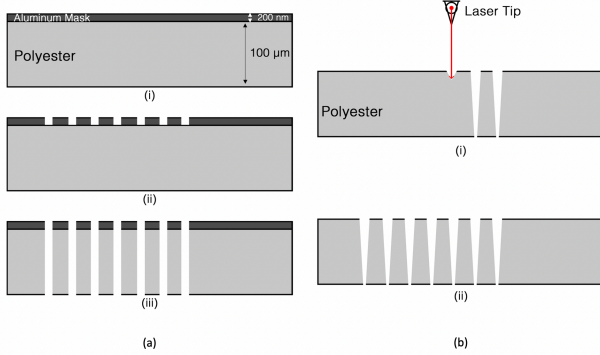


Figure 7: (a) Brief fabrication steps with  $\text{O}_2$  RIE: (i) sputter-deposit  $200\text{ nm}$  thick Al on  $100\text{ }\mu\text{m}$  thick polyester sheet, (ii) wet etch Al after photolithography, (iii) use RIE to etch polyester to form orifice; (b) fabrication with laser cutter: (i) use laser cutter to etch out orifices by controlling exposure power and radiation time, (ii) conical cross-sectional view of the orifices obtained with the laser cutter.

The etch rate of the polyester with oxygen plasma in RIE is found to be non-linear due to polyester etch-byproducts filling up the orifices. The orifices fabricated with RIE have vertical sidewalls (Fig. 7a(iii)), though the orifices made with a laser cutter have cone-shaped sidewalls (Fig. 7b(ii)). Orifice fabrication with a laser cutter is done over various thick polyester sheets by controlling the laser power and radiation time (Fig. 7b(i)). But the orifices by the laser cutter have conical cross-section due to thermal effects of the laser beam (Fig. 7b(ii)).

The cross sections of the orifices have been obtained by dicing

the substrates with a Dicing Saw, and their images obtained with a microscope are shown Fig. 8. For the orifices with conical sidewalls, the side with larger diameter is aligned to face the speaker, the sound source.

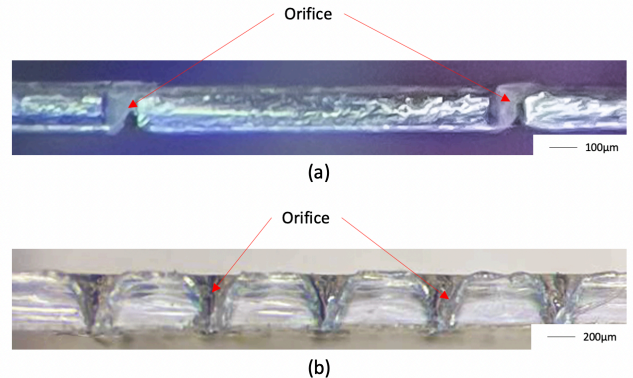


Figure 8: Cross sectional images of the orifices fabricated by (a) RIE showing vertical sidewalls, (b) a laser cutter showing conical sidewall

The laser-machined orifices have produced higher acoustic propulsion in both audible and ultrasound range. The device with  $100\text{-}\mu\text{m-diameter, } 100\text{-}\mu\text{m-thick}$  orifices made by a laser cutter produces a peak of  $5.4\text{ mg}$  propulsion over ultrasound range (at  $66\text{ kHz}$ ), about two times larger than the highest obtained over ultrasound range with the orifices made with RIE. Over the audible range, the orifices fabricated with a laser cutter performed far better than the ones made with RIE (Fig. 9). Based on our experiments, it is evident that for better acoustic propulsion, it is better to have orifice designs having conical structure to allow for acoustic focusing.

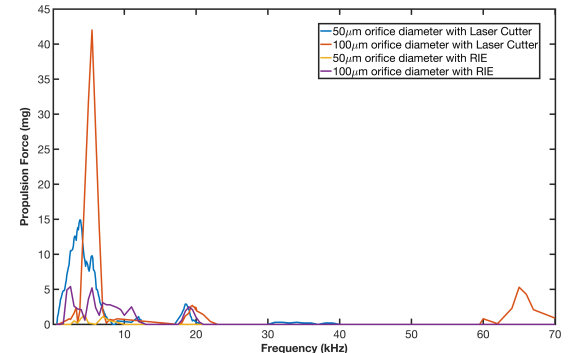


Figure 9: Measured propulsion force vs frequency with different orifices made with a laser cutter and RIE on  $100\text{ }\mu\text{m}$  thick polyester sheets.

### Temperature effect

As the speaker generates heat which strongly dependent on the applied frequency and voltage (with a higher frequency and higher voltage leading to faster temperature rise, according to Figs. 10 and 11), the acoustic propulsion force has been characterized. Although high temperature can damage the speaker; the temperature rise increases the propulsion force at some frequencies, though it decreases at some other frequencies, depending on the orifice design (Fig. 12), indicating that higher propulsion force can be achieved through proper temperature control.

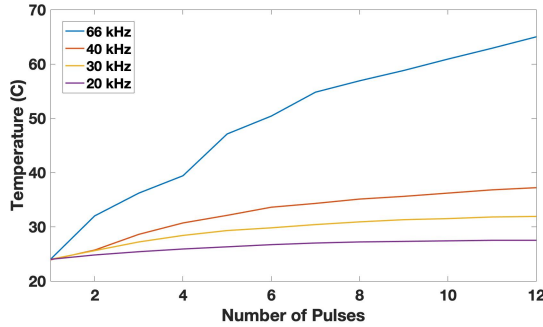


Figure 10: Speaker temperature vs the number of pulses as a function of sinusoidal frequencies (with  $20V_{pp}$ , 40% duty cycle).

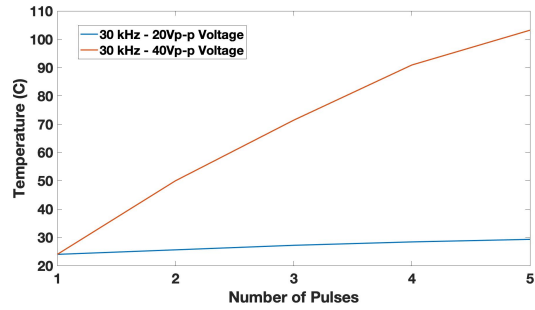


Figure 11: Speaker temperature vs the number of pulses as a function of voltage applied (with 30 kHz, 40% duty cycle).

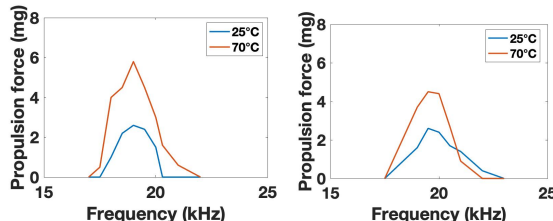


Figure 12: Propulsion forces vs frequency at 25 and 70 °C for the propeller (a) with 0.1 mm thick orifices of 100  $\mu\text{m}$  in diameter and (b) with 0.1 mm thick orifices of 50  $\mu\text{m}$  in diameter.

### Propulsion phenomena

The propulsion forces generated by ultrasounds (without any audible sound) are shown to make the propellers jump and move laterally at about several mm/sec (Fig. 13).

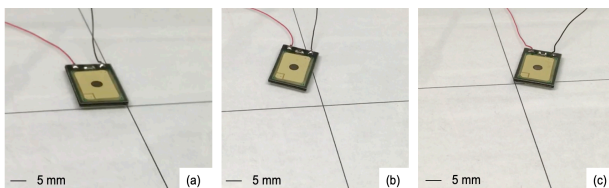


Figure 13: Photos showing movement of the propeller (with 100  $\mu\text{m}$  thick orifices of 100  $\mu\text{m}$  in diameter): (a) before power on, (b) 1 sec after 20 kHz, 20  $V_{pp}$ , (c) 1 sec after 66 kHz, 20  $V_{pp}$ .

### SUMMARY

The propulsion forces generated through synthetic jets with airborne ultrasound are measured quantitatively through a precision scale, as the orifice parameters are varied. Among the parameters we have explored, the orifices with 100  $\mu\text{m}$  thickness and 100  $\mu\text{m}$  in diameter produce the highest propulsion force. Orifices with conical sidewall (obtained with laser drilling) are shown to produce higher acoustic propulsion force than orifices with vertical sidewall, when the side with a larger orifice opening faces the speaker. Also, temperature rise is found to have significant effect on propulsion force and may advantageously be used for enhancing propulsion force.

### ACKNOWLEDGEMENTS

This paper is based on the work supported by National Science Foundation under grant ECCS2017926.

### REFERENCES

- [1] A. P. Thomas, M. Milano, M. G. G'Sell, K. Fischer and J. Burdick, "Synthetic Jet Propulsion for Small Underwater Vehicles," Proceedings of the 2005 IEEE International Conference on Robotics and Automation, 2005, pp. 181-187
- [2] S. J. Campbell, W. Z. Black, A. Glezer and J. G. Hartley, "Thermal management of a laptop computer with synthetic air microjets," ITherm'98. Sixth Intersociety Conference on Thermal and Thermomechanical Phenomena in Electronic Systems (Cat. No.98CH36208), 1998, pp. 43-50
- [3] I. Wygnanski, and I. Wygnanski. "Boundary layer and flow control by periodic addition of momentum." In 4th Shear Flow Control Conference, p. 2117. 1997.
- [4] U. Ingård, and S. Labate. "Acoustic circulation effects and the nonlinear impedance of orifices." The Journal of the Acoustical Society of America 22, no. 2 (1950): 211-218.
- [5] M. Chiatto, "Design and Performance Evaluation of Piezo-Driven Synthetic Jet Devices." World Journal of Engineering and Technology 4, no. 03 (2016): 107.
- [6] M. Mueller, L. Bernal, P. Miska, P. Washabaugh, T.-K. Chou, B. Parviz, C. Zhang, and K. Najafi. "Flow structure and performance of axisymmetric synthetic jets." In 39th Aerospace Sciences Meeting and Exhibit, p. 1008. 2001.
- [7] M. Mueller, L. Bernal, R. Moran, P. Washabaugh, B. Parviz, T.-K. Chou, C. Zhang, and K. Najafi. "Thrust performance of micromachined synthetic jets." In Fluids 2000 Conference and Exhibit, p. 2404. 2000.
- [8] Y. Tang, and E.S. Kim. "Acoustic Propeller Based on Air Jets from Acoustic Streaming." In 2019 20th International Conference on Solid-State Sensors, Actuators and Microsystems & Eurosensors XXXIII (TRANSDUCERS & EUROSENSORS XXXIII), pp. 2068-2071. IEEE, 2019.

### CONTACT

\*Hai Liu, tel: +1-213-709-3516; [hailiu@usc.edu](mailto:hailiu@usc.edu)